

# Model sensitivity to MACC anthropogenic and biogenic emissions: Global simulations and evaluation for reactive gases

Olaf Stein, Martin G. Schultz, Angelika Heil  
Research Centre Jülich, 52425 Jülich, Germany

[o.stein@fz-juelich.de](mailto:o.stein@fz-juelich.de)

Idir Bouarar  
L'Atmos, UPMC Paris, France

Hannah Clark  
Météo France, CNRM, Toulouse, France

Eleni Katragkou  
Aristotle University of Thessaloniki, Greece

Joana Leitao  
IUP, University Bremen, Germany

## ABSTRACT

A global emission inventory for reactive gases has been developed as part of the European project MACC (Monitoring Atmospheric Composition and Climate). ACCMIP emissions were extrapolated for years after 2000 with the RCP8.5 scenario and extended for VOCs and several other species. This inventory composes the MACCcity anthropogenic emission inventory.

During the MACC project it became apparent that using MACCcity in reanalysis simulations for recent years led to an underestimation of CO concentrations in the Northern Hemisphere when compared to independent observations. We conducted MOZART offline simulations for the year 2008 to test the sensitivity of a global chemical transport model to the varying emissions. Therefore we ran MOZART with different sets of emissions: 1. MACCcity emissions, 2. The GEMS/RETRO emission inventory, 3. MACCcity emissions, but with increased traffic CO emissions. While using the emission inventory developed in RETRO gives quite reasonable tropospheric concentrations for the key species, the MACCcity CO emissions are too low, particularly during NH winter. When increasing MACCcity CO traffic emissions by a constant factor, the simulations result in a better representation of surface and satellite observations for Europe, but not for other parts of the world. A refined scaling needs to be applied to the inventory which enhances anthropogenic CO and VOC emissions significantly. Increasing biogenic emissions result in unrealistic high summer concentrations and are therefore not considered as potentially missing sources. The results point to significant underestimation of traffic CO emissions in the MACCcity emission inventory, which is potentially amplified by an unrealistic emission reduction 2000-2010 in the RCP8.5 scenario.

## INTRODUCTION

Carbon monoxide (CO) is a product of incomplete combustion and is also produced from oxidation of volatile organic compounds (VOC) in the atmosphere. It is of interest as an indirect greenhouse gas and an air pollutant causing health effects and is thus subject to

emission restrictions. CO acts as a major sink for the OH radical and as a precursor for tropospheric ozone and affects the oxidizing capacity of the atmosphere via its influence on the budget of OH. Due to its mean tropospheric lifetime of about two months CO is often used as a tracer for long-range pollution transport.

The main CO sources are from anthropogenic and natural direct emissions, mostly fossil fuel and biomass burning together with smaller contributions from vegetation and the oceans, as well as oxidation of methane and VOCs. Automobile traffic causes 85-90% of the CO fossil fuel emissions, but the strength of this source is decreasing since the 1990s for the industrialized countries (e.g. Miller et al. 2008). The reaction with OH acts as the major CO sink, while deposition in soils contributes about 10% to the global CO sink. The current tropospheric CO abundances reach from 50 ppb in the remote Southern Hemisphere to 220 ppb for wintertime Northern Hemisphere background mixing ratios and 60 ppb in summer, when more OH radicals are available as reaction partners. Above and downwind of strong polluted areas the mean tropospheric concentrations can reach more than 1000 ppb during winter. The atmospheric burden is about 360 Tg.

It is long known that both global chemistry transport models (CTM) and chemistry climate models (GCM) have problems in modelling the correct amount of present-day CO in the atmosphere. Shindell et al. (2006) reported large underestimates in extratropical Northern Hemisphere (NH) CO when comparing 26 global models to surface and satellite observations. They suggested a severe underestimation of East Asia anthropogenic emissions and African biomass burning emissions in the available emission inventories. Several studies have used inverse modelling techniques to constrain the CO sources from observations (e.g. Bergamaschi et al. 2000a, 2000b; Kasibhatla et al. 2002; Pétron et al. 2002, 2004; Arellano et al. 2005, 2006; Müller and Stavrou 2005; Kopacz et al. 2010; Fortems-Cheiney et al. 2011; Hooghiemstra et al. 2012). Most of these inversions resulted in significantly higher CO a-posteriori emissions than the current bottom-up inventories imply.

In the following we will show how the emission uncertainties effect global model simulations which employ chemical data assimilation and perform CTM sensitivity studies to identify possible missing emission sources for CO and VOCs both on the global and on the regional scale.

## MODEL SETUP

The EU FP7 projects MACC (Monitoring Atmospheric Composition and Climate, 2009-2011) and MACC-II (2011-2013) prepare for the operational Global Monitoring for Environment and Security (GMES) atmospheric core service on greenhouse gases, reactive gases and aerosols which is envisaged to start in 2014.

The meteorological forecast and data assimilation system IFS (Integrated Forecast System, <http://www.ecmwf.int/research/ifsdocs>) at the European Centre for Medium-Range Weather Forecast (ECMWF) has been coupled to an updated version of the global chemistry transport model MOZART-3 (Model for Ozone And Related Tracers, version 3; Kinnison et al. 2007) in order to build the coupled MACC system MACC-IFS-MOZ (Flemming et al. 2009). For a coupled simulation both models are running in parallel and exchange several two- and three-dimensional fields every hour using the OASIS4 coupling software developed in the PRISM project (Valcke & Redler 2006). Data assimilation of the MACC species O<sub>3</sub>, CO, NO<sub>x</sub>, HCHO, and SO<sub>2</sub> takes place in IFS, which provides basic meteorological data and species initial concentrations to MOZART. Chemical reaction equations, emissions and deposition are calculated in MOZART. Transport processes are parameterized in both models. MOZART provides updated tendency terms for chemistry, emission and deposition sources and sinks for the MACC species, which are then used to constrain the data assimilation in the

next cycle. MOZART uses the same 60 vertical hybrid layers as in current IFS simulations reaching from the surface to 0.1 hPa. The MOZART system of chemical reactions consists of 115 species, 71 photolysis reactions, 223 gas phase reactions and 21 heterogeneous reactions. The MACC reanalysis (Inness et al. 2012) and the forecasts performed in near real time (NRT) benefit from the multi-sensor approach for data assimilation of total columns, tropospheric columns, and vertically resolved satellite observations of ozone, CO and NO<sub>2</sub> (Stein et al. 2012). The MACC reanalysis covers the period 2003-2011 with an IFS spectral resolution of T255 corresponding to a horizontal resolution of about 80 km. The MOZART resolution is 1.125°x1.125°. In spite of the extensive satellite data assimilation modelled tropospheric concentrations are still not always satisfactory. Apart from biases and missing near-surface sensitivity in the satellite retrievals there also still exists considerable uncertainty on surface emissions. We will show CO concentrations 2003-2010 from the MACC reanalysis and a control simulation without data assimilation run in parallel to the reanalysis. Sensitivity studies with varying emissions for the year 2008 have been conducted with the MOZART CTM in a standalone version. For these simulations MOZART was driven by meteorological fields from the ECMWF ERA INTERIM reanalysis (Dee et al. 2011) and accomplish a horizontal resolution of 1.875° x 1.895° with the same vertical levels than for the MACC model.

A new inventory of global anthropogenic emissions has been developed in the MACC and CITYZEN projects (Granier et al. 2011) which provides up-to-date estimates for use in the global MACC models (MACCcity). These emission estimates are based on the ACCMIP emissions for the year 2000 (Lamarque et al. 2010). The 2000-2011 MACCcity emissions were obtained by using the 2005/2010/2015 emissions from the future scenario RCP8.5 (Representative Concentration Pathway): a linear interpolation was applied to obtain the yearly MACCcity emissions. RCP8.5 corresponds to a radiative forcing of 8.5 W m<sup>-2</sup> in 2100 given the respective emissions (Moss et al. 2010; van Vuuren et al. 2011; Riahi et al. 2011). A source-specific seasonality developed for the RETRO project ( <http://retro.enes.org/> ) was applied to the emissions.

Ship emissions are from Eyring et al. (2010), biogenic emissions from a recent update (Barkley, 2010) of MEGAN-v2 (Guenther et al. 2006, <http://acd.ucar.edu/~guenther/MEGAN/MEGAN.htm> ) and other natural emissions are from the POET project (Granier et al. 2005) and GEIA. The anthropogenic emissions from these inventories are also available on the GEIA-ACCENT emission data portal <http://www.geiacenter.org/>.

The MACCcity emissions 2003-2010 have been used in the MACC reanalysis and the control simulation without data assimilation. These are also used as reference emissions for MOZART 2008 sensitivity simulations.

Biomass burning emissions in the MACC reanalysis for the years 2003-2008 are generated from the Global Fire Emissions Database, version 3.0 (GVEDv3.0; van der Werf et al. 2010) and the Global Fire Assimilation System (GFAS) by using GFAS to create daily gridded Fire Radiative Power (FRP) maps with which the monthly GFED emissions were redistributed amongst the days of each month (Kaiser et al. 2011). For 2009 and 2010, daily biomass burning emissions were derived from the GFASv1 product (Kaiser et al. 2012). A preliminary version of GFASv1 was also used for all MOZART 2008 simulations described here.

An alternative emission inventory applied for one of the MOZART simulations was compiled for the GEMS project (Hollingsworth et al. 2008) derived from emissions out of the EU FP6 project RETRO (Schultz et al. 2007; data available from [http://retro.enes.org/data\\_emissions.shtml](http://retro.enes.org/data_emissions.shtml)) merged with updated emissions for East Asia (REAS inventory, Ohara et al. 2007). These emissions are in the following called RETRO/REAS. Anthropogenic and natural emissions are provided as monthly mean fields

representing the year 2003. Biogenic emissions in RETRO are derived from a decadal data set of Lathiere et al. (2005). Emissions of SO<sub>2</sub>, NH<sub>3</sub>, and DMS are not part of the RETRO inventory and have been taken from various sources: SO<sub>2</sub> anthropogenic emissions are from EDGAR-FT2000 (Olivier et al. 2005), SO<sub>2</sub> volcano emissions from GEIA (<http://www.geiacenter.org/>), NH<sub>3</sub> emissions from EDGAR2 (Olivier et al. 1996), and DMS emissions from Kloster et al. (2006). The RETRO ship emissions have been replaced by estimates based on Corbett et al. (2003) and East Asian anthropogenic emissions have been replaced by the REAS inventory (Ohara et al. 2007) but keeping the original RETRO seasonality.

## RESULTS FROM THE MACC REANALYSIS

After the MACC reanalysis had been started it became apparent that using the MACCity emissions led to an underestimation of CO concentrations in the Northern Hemisphere compared to independent observations. Figure 1 shows the zonal mean CO total column densities from MOPITT and IASI satellite observations, the MACC reanalysis, and the reanalysis control run.

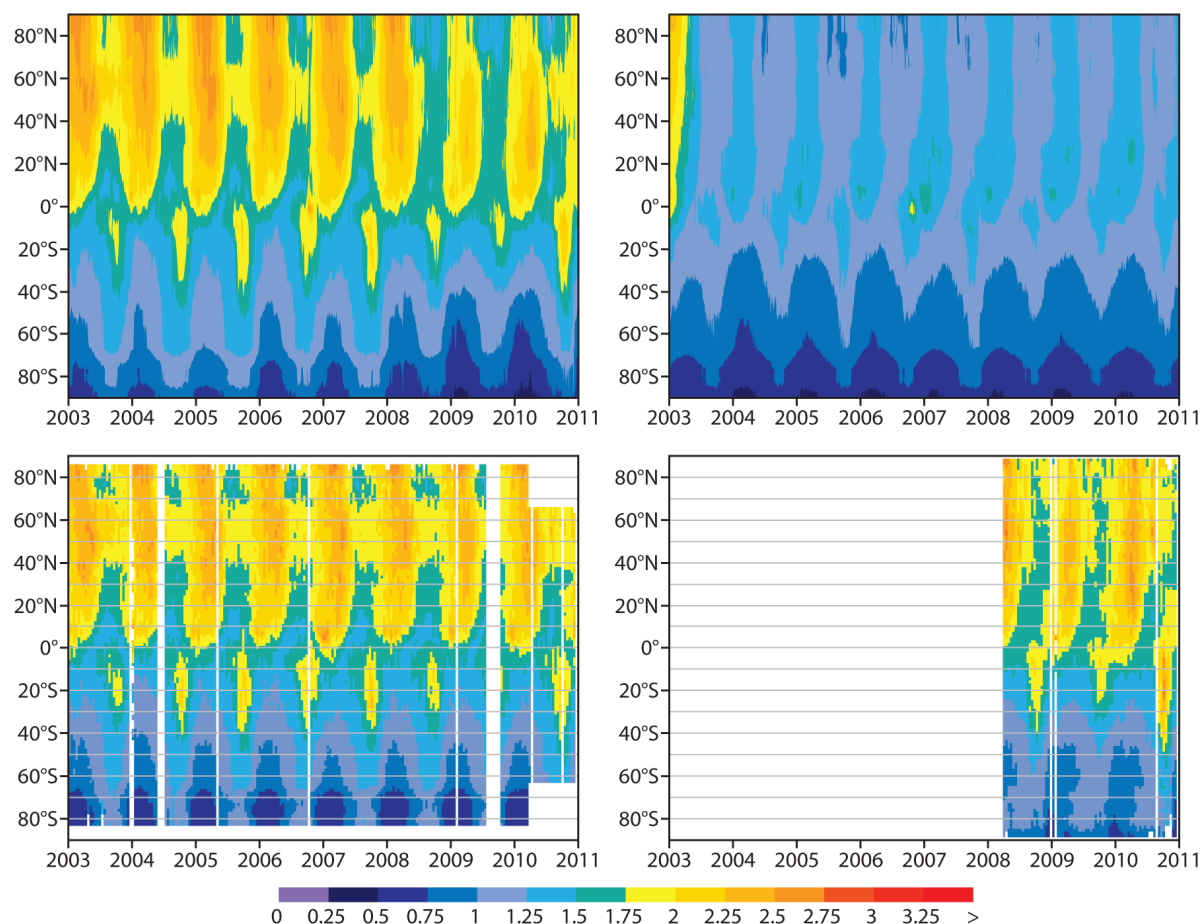


**Figure 1.** Timeseries of zonal mean total column CO field in 1018 molec/cm<sup>2</sup> for the period 2003 to 2010 from the MACC reanalysis (top left), the control run (top right), MOPITT (bottom left) and IASI (bottom right). The MOPITT timeseries shows the change to NRT data in 2010, for which no data are available polewards of 65°.

While the data assimilation in the MACC reanalysis draws the modelled values to the observations, the total columns in the control run are far too low compared to MOPITT. Similar discrepancies can be seen when comparing the surface level model concentrations to NOAA/GMD surface observations (Figure 2).

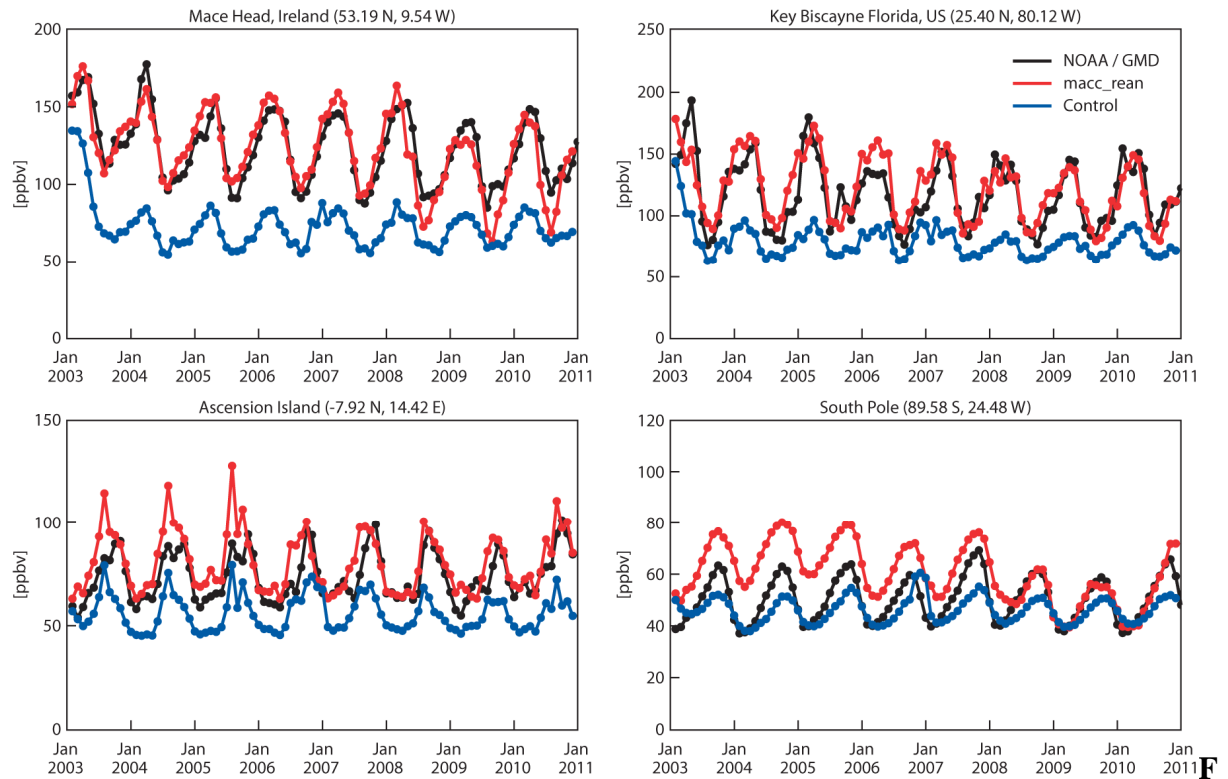


**Figure 2.** Time series of monthly mean CO concentrations (ppbv) from the reanalysis (red), the control run (blue), and from NOAA/GMD ground-based measurements (black) for four stations from the NOAA/GMD network.

The control run shows largest negative biases during NH winter and spring. Even with data assimilation lower tropospheric CO concentrations in the reanalysis are 10-20% low compared to MOZAIC vertical profiles at several airports as shown in Figure 3.

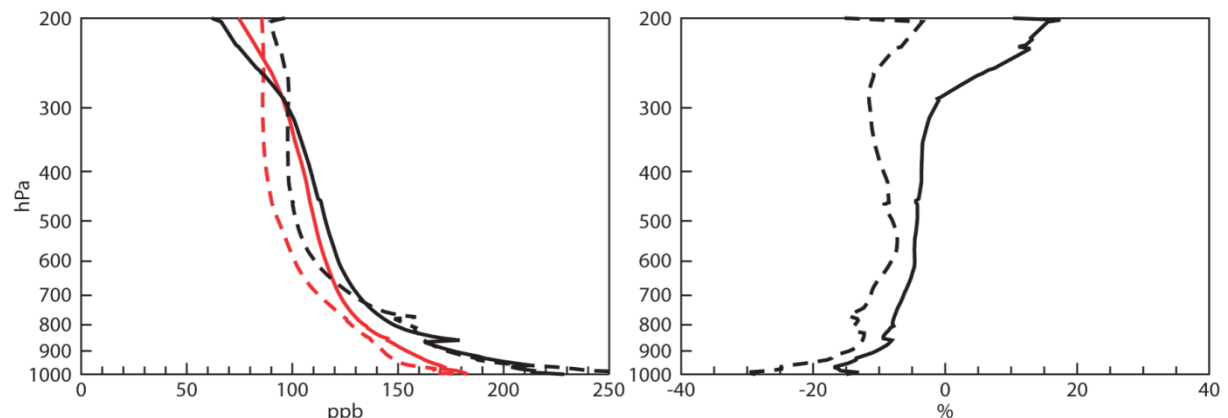


**Figure 3.** Left panel: Mean CO profiles 2003-2010 from the MACC reanalysis (red) and MOZAIC data (black). The solid lines show the means for NH airports (north of 30°N), the dashed lines the means for tropical airports (30°S-30°N). Right panel: CO bias (MACC reanalysis - MOZAIC).

The assimilated CO satellite data have only little sensitivity to concentrations in the lower troposphere, where the influence of the emissions gets more important. In the following we use MOZART standalone simulations to identify the role of the various CO sources for the underestimation problem.

## MOZART SENSITIVITY SIMULATIONS

In this section sensitivity simulations performed with the MOZART model will be presented and evaluated with CO station data and satellite total columns. The simulations differ by their used emission inventories and are summarized in Table 1.

**Table 1.** Description of MOZART model simulations for the year 2008

simulation	Anthropogenic emissions	Biogenic emissions
RR	RETRO/REAS	Lathiere et al. (2005)
MI	MACCity	MEGANv2.0
MI+	MACCity, CO traffic emissions scaled by a factor of 2.5	MEGANv2.0
MI+NA_EU	MACCity, CO traffic emissions scaled for Europe and North America	MEGANv2.0
MI+VOC	MACCity, VOC anthropogenic emissions doubled	MEGANv2.0
MI+BIO	MACCity, CO and VOC biogenic emissions doubled	MEGANv2.0, CO and VOC emissions doubled

All model simulations are for the year 2008 but starting at July 1, 2007 to overcome disturbances during the onset period. The model is run at T63LR resolution ( $1.875^\circ \times 1.895^\circ$ ) and with 60 vertical levels from the surface up to 0.1 hPa. Meteorology is from the ERA INTERIM reanalysis while tracer initial conditions are taken from the MACC reanalysis which itself also includes assimilation of CO, O<sub>3</sub>, and NO<sub>2</sub> column densities.

RETRO/REAS and MACCity anthropogenic CO emissions differ with regard to the emission patterns (Figure 4) and the global emission totals (Table 2). Most notably, MACCity emissions are lower over the highly populated areas of North America and Central Europe.

**Table 2.** 2008 Emission totals in Tg/y for RETRO/REAS and MACCity inventories for selected species. NO<sub>x</sub> emissions are expressed as Tg NO / y. Biomass burning emissions are always from GFASv1.

	RETRO/REAS			MACCity		
	CO	NO <sub>x</sub>	HCHO	CO	NO <sub>x</sub>	HCHO
<b>anthropogenic</b>	575.2	68.4	1.17	585.2	70.3	3.37
<b>biogenic</b>	159.9		25.3	76.2		4.01
<b>other natural</b>	19.9	20.0		19.9	10.6	
<b>total</b>	755.0	88.4	26.5	681.3	80.9	7.38
<b>biomass burning</b>	322.9	9.28	4.92	322.9	9.28	4.92

The more recent MACCity inventory reflects the emission reduction efforts made in the industrialized countries except for China and other parts of East Asia where emissions have not been reduced due to excessive economic growth and rising prosperity. Similar pattern shifts are also found for most other emitted species (not shown) which are typically connected to CO emissions by an emission factor dependent on the emission sector or on the surface vegetation type.

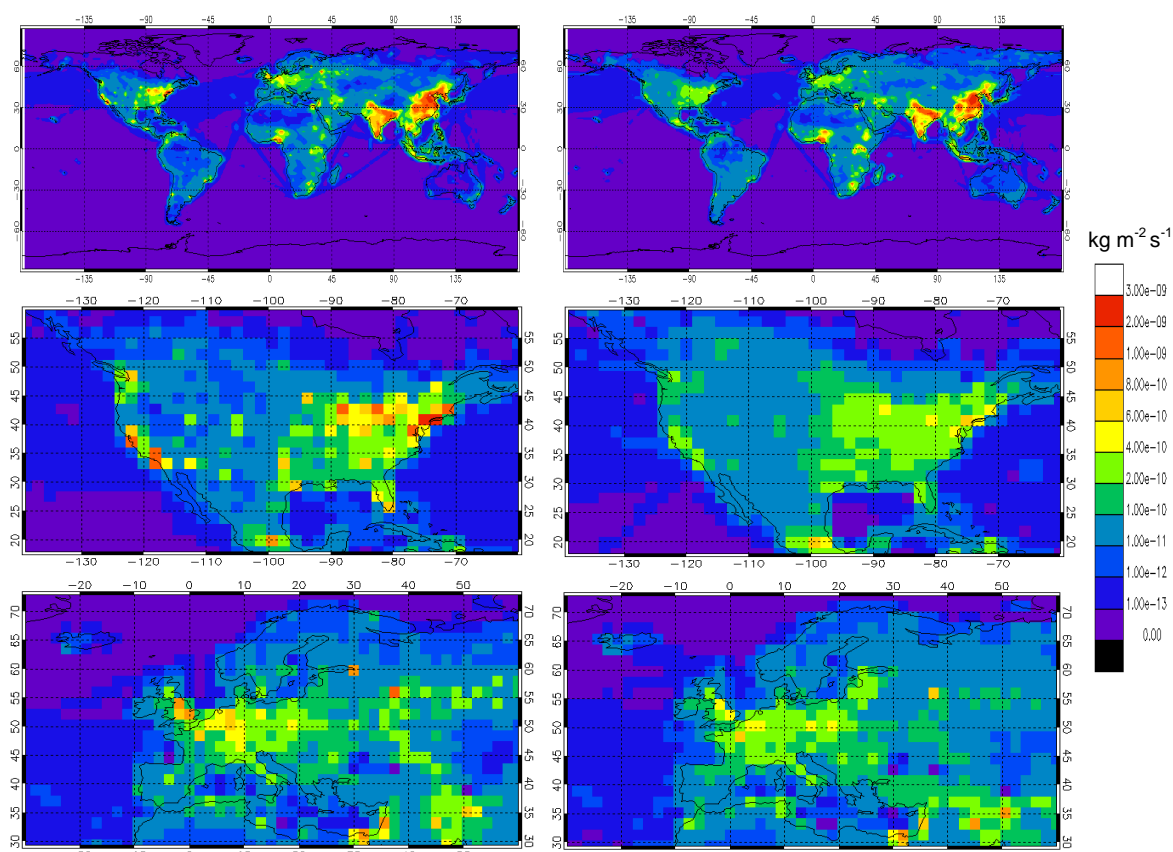


**Figure 4.** Mean CO anthropogenic emission fluxes from RETRO/REAS (left) and from MACCity for 2008 (right). Top: global view, middle: North America, bottom: Europe. Units are  $\text{kg}(\text{CO}) \text{m}^{-2} \text{s}^{-1}$

In the case of CO and most other species natural emissions are dominated by the biogenic emissions which are most prominent over the tropical and moist subtropical landmasses. Figure 2 shows the differences between RETRO/REAS and MACCity natural CO emissions. In general, CO biogenic emissions from MACCity are much lower than those from RETRO/REAS, reflecting the lower estimates from the MEGANv2 model (Table 2). Also shifts in the position of local maxima and minima are to be mentioned, particularly striking over tropical South America.

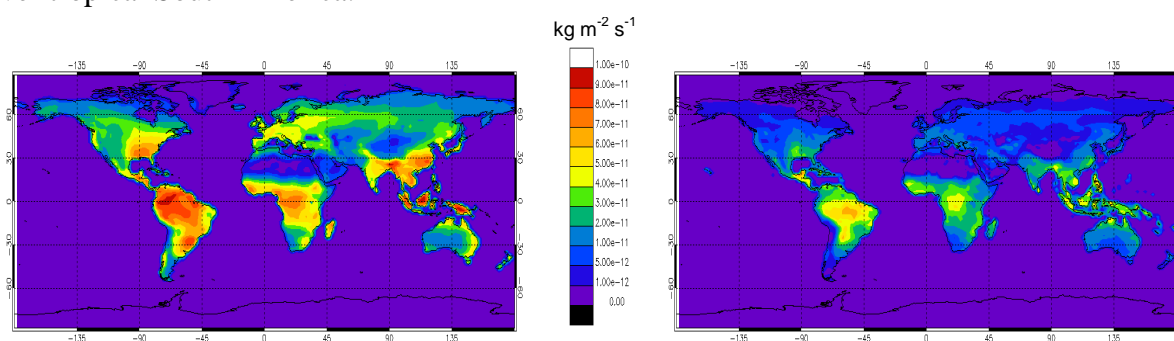


**Figure 5.** Mean CO natural emission fluxes from RETRO/REAS (left) and from MACCity (right). Units are  $\text{kg}(\text{CO}) \text{m}^{-2} \text{s}^{-1}$

Tropospheric CO builds up over the Northern Hemisphere during wintertime, when emissions are high and photochemical activity is low. The surface CO concentrations peak around March with typical mixing ratios measured at background stations of around 150 ppb.

We compared monthly means of model concentrations to surface station data available from the World Data Center for Greenhouse gases (WDCGG) database for the Northern

Hemisphere and for the regions Europe (30°W-45°E, 30°N-90°N), North America (130°W-45°W, 20°N-60°N) and East Asia (100°E-160°E, 20°N-50°N). Model data was interpolated to the station location. In Figure 6 the comparison is shown for the three basic simulations RR, MI and MI+.

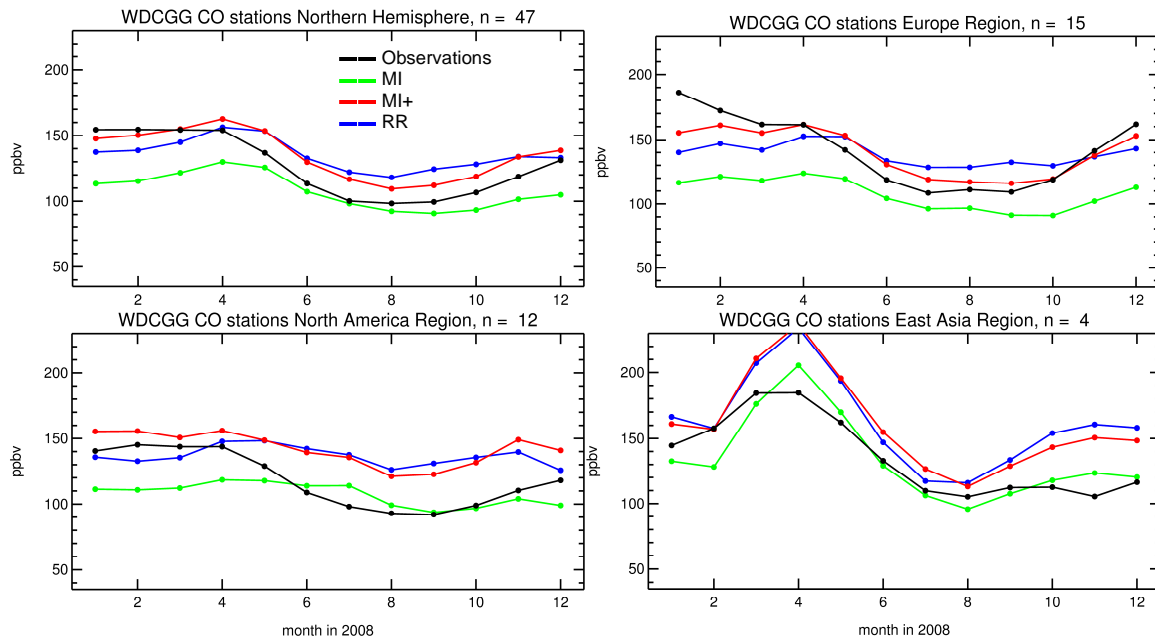


**Figure 6.** Modelled 2008 monthly mean surface level mixing ratios from three MOZART simulations with varying emissions compared to observations from WDCGG. n denotes the number of stations used.

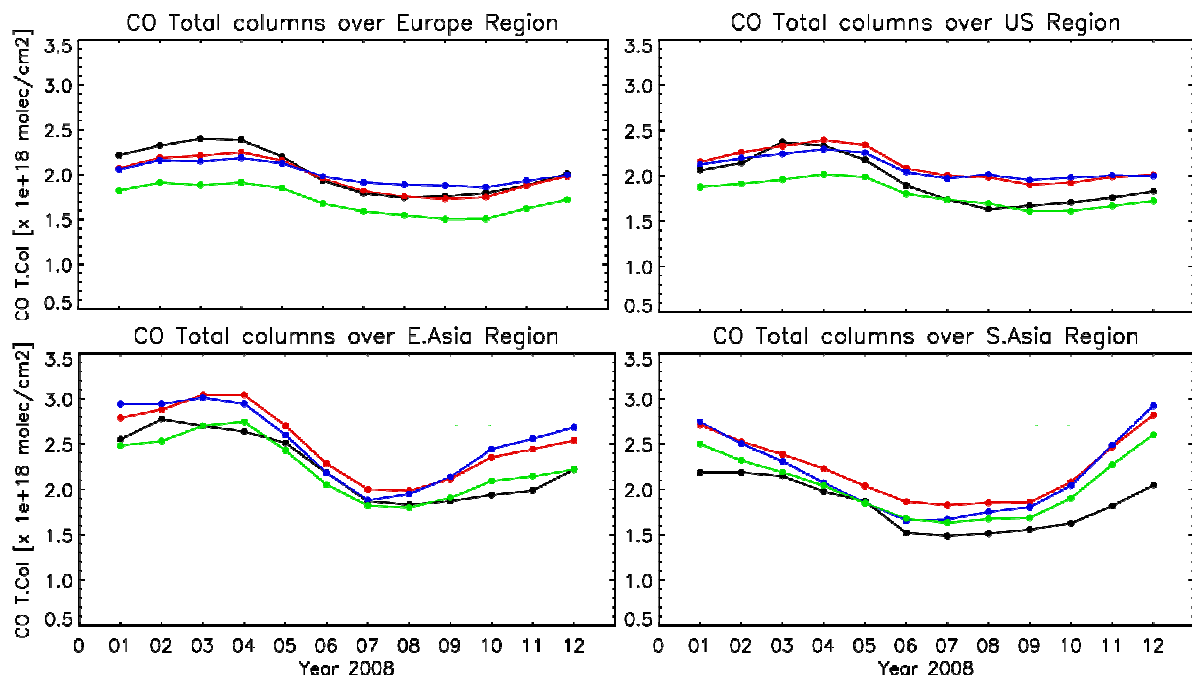


**Figure 7.** Modelled 2008 monthly mean CO total columns from three MOZART simulations with varying emissions compared to observations from MOPITT. MOPITT averaging kernels were taken into account when calculating the model total columns.

Similarly, the modelled CO total columns are compared to MOPITTv3 total column observations (Figure 7). The simulation with emissions from the RETRO/REAS emission inventory (blue lines) generally match the observed CO concentrations on a global scale in wintertime, but has too high values in summer and autumn, particularly over North America. Also European concentrations during wintertime are underestimated. East Asian emissions are overestimated for almost the whole year. It has to be taken into account that the RETRO/REAS emissions were built for the base year 2003. Since then it is assumed that anthropogenic emissions of short-lived pollutants have decreased with tightened air quality legislation in the developed countries. This is included in the more recent MACCity emission inventory for 2008: The MI simulation (green line) shows generally lower CO concentrations than the RR simulation. Compared to the observations, though, the MI simulation is too low in all seasons except summer with largest low biases of about 70 ppb in January over Europe. The East Asian region is exceptional as the observed concentrations seem to be simulated quite well by the MI simulation, which is probably due to updated emission information for China in the MACCity inventory.

As indicated in section 2, the MACCity inventory for the base year 2000 is based on ACCMIP emissions combined with EPA data for USA, EMEP data for Europe, and REAS data for East Asia. Based on a comparison between a fuel-based and a mileage-based emission inventory for one US city Parrish (2006) concluded that the reason for a high bias in the CO to NO<sub>x</sub> ratios in the US National Emission Inventory (NEI) was most likely due to an overestimate of the CO emissions rather than an underestimate in the NO<sub>x</sub> emissions and suggested an overestimate of CO emissions (by a factor of 2) in the EPA-2004 data, which also holds true for the more recent EPA estimates up to 2008 (Lamarque et al. 2010, Granier et al. 2011). EPA also reported on air pollution trends of US cities between 1990 and 2008 and found maximal decadal decreases in CO pollution for US cities of 60 to 80% for 1990 to 2008 (Riahi et al. 2011). In the RCP8.5 scenario an exposure-driven spatial algorithm for the downscaling of the regional emission projection has been employed leading to the highest emission reduction of up to 80% per decade in those grid cells with the highest exposure for regions where emissions are reduced due to air pollution measures, e.g. USA and Europe. For regions with increasing emissions (e.g. in Asia) emissions increase proportionally to the acceleration of the economic activity (Riahi et al. 2011). In Figure 8 the development of CO road traffic emissions 2000-2100 for the different RCP scenarios is shown: Although RCP8.5 is a scenario with relatively high greenhouse gas emissions and global warming potential, the CO anthropogenic emissions decrease rapidly in the first decade, mostly driven by the emission reduction in the OECD countries. Traffic emissions, which build the majority of anthropogenic CO emissions from these countries decrease from 120 Tg/y in 2000 to 40 Tg/y in 2010).

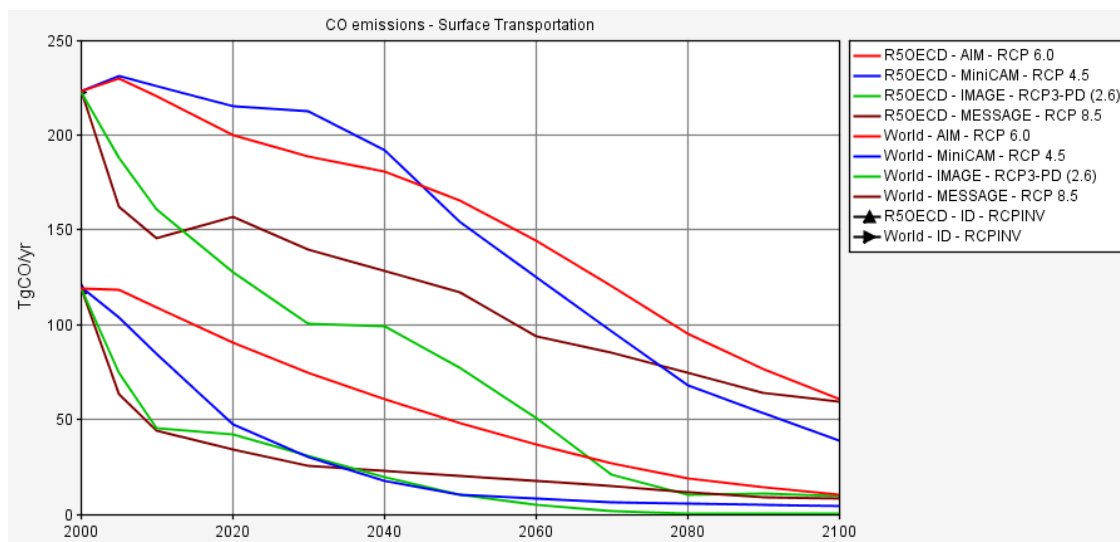


**Figure 8.** CO emissions from the surface transportation sector in the RCP scenarios, world-wide and for OECD countries, RCP8.5 scenario in brown.

The simulation MI+ tests for the hypothesis that CO emissions from cars are not considered adequately in the MACCity estimate: Estimates of automobile emissions are based on defined driving cycles which are lacking of typical short trips, when much more CO is emitted under cold engine conditions (Parrish 2006). This would effect a significant underestimation of traffic CO emissions in the emission inventory, which is potentially amplified by an unrealistic emission reduction 2000-2010 in MACCity.

Indeed, multiplying the MACCity traffic emissions by a factor of 2.5 leads to a much better representation of the absolute values and annual variation for surface background stations for Europe and partly for North America, but not for other regions, where the resulting concentrations are too high (Figures 6 and 7). Furthermore, summertime concentrations from this simulation are always biased high. In another sensitivity simulation we therefore applied an optimized scaling to the CO traffic emissions with the following monthly scaling factors for Europe and North America (simulation MI+NA\_EU), which enhance wintertime CO only for these regions (Table 4):

**Table 4.** monthly scaling factors for CO traffic emissions over Nort America and Europe as applied in simulation MI+NA\_EU

	Jan	Feb	Mar	Apr	May	Jun	Jul	Aug	Sep	Oct	Nov	Dec
North America	2	2	2	2	1	1	1	1	1	1	1	2
Europe	3	2.875	2.75	2.625	2.5	1.5	1.5	1.5	2	2.5	2.67	2.83

Comparison to surface observations from simulation MI+NA\_EU is shown in Figure 9 (magenta lines). This simulation is able to shift wintertime CO concentrations to higher values for Europe and North America without increasing East Asian concentrations by a large extent. To account for the uncertainties in CO precursor emissions, we also ran MOZART with MACCity emissions and VOC anthropogenic emissions doubled (MI+VOC). These increased emissions also enhance wintertime CO concentrations by up to 10 ppb (Figure 9, brown lines). When doubling biogenic CO and VOC emissions (simulation MI+BIO) the CO

concentrations also increase significantly, but leading to unrealistically high concentrations during summer (Figure 9, turquoise lines). We therefore do not consider these emissions responsible for the NH wintertime CO underestimation.

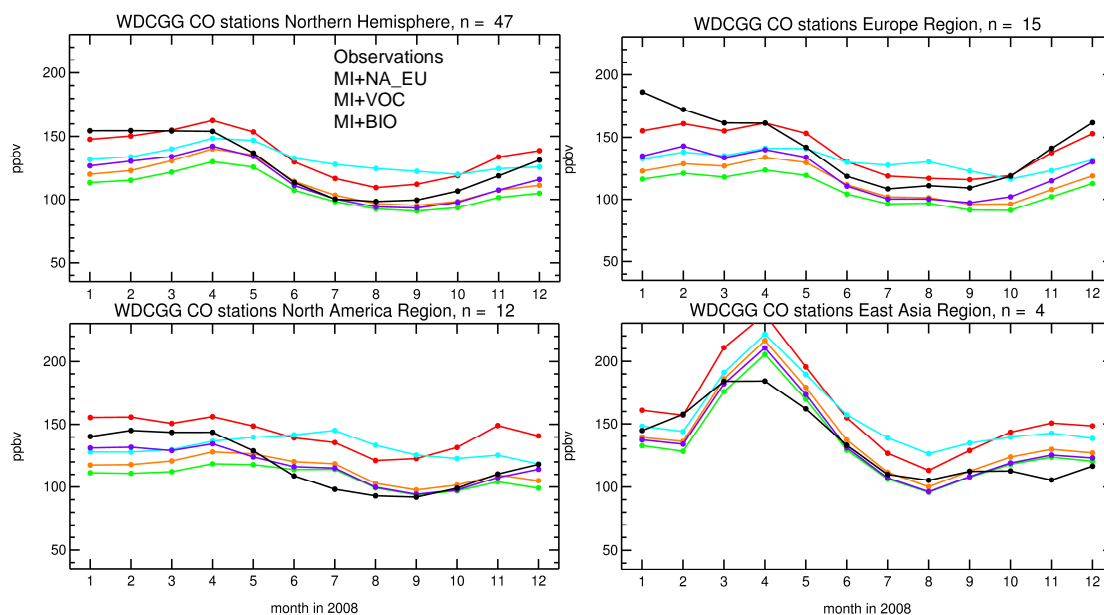


**Figure 9.** As Figure 6, but now additionally for simulations MI+NA\_EU, MI+VOC and MI+BIO

## CONCLUSIONS

The problem of missing NH wintertime CO concentrations, which is apparent in most global model simulations is likely due to missing emissions of anthropogenic CO and VOCs in current emission inventories. In comparison to other emission inventories like EDGARv4.2, EPA, GAINS, TNO, EMEP, MACCity seems to underestimate emissions from industrialized countries, except for East Asia. Estimates for emission reduction in recent years may be too optimistic and do not account properly for the developments in the emerging countries. Furthermore, research efforts are also needed to improve the estimates for seasonal variation of anthropogenic emissions. For a proper representation of CO observations with MOZART global model simulations significant amounts of additional anthropogenic sources from CO or VOCs need to be added to the existing emission inventories, preferably for Europe and North America.

## ACKNOWLEDGEMENTS

This study was funded by the European Commission under the framework programme 7 (contract number 218793).

## REFERENCES

Arellano, A. F., Jr., P. S. Kasibhatla, L. Giglio, G. R. van der Werf, and J. T. Randerson (2004), Correction to “Top-down estimates of global CO sources using MOPITT measurements”, *Geophys. Res. Lett.*, 31, L12108, doi:10.1029/2004GL020311.

Arellano, A. F., Jr., P. S. Kasibhatla, L. Giglio, G. R. van der Werf, J. T. Randerson, and G. J. Collatz (2006), Time-dependent inversion estimates of global biomass-burning CO emissions using Measurement of Pollution in the Troposphere (MOPITT) measurements, *J. Geophys. Res.*, 111, D09303, doi:10.1029/2005JD006613.

Barkley, M.: Description of MEGAN biogenic VOC emissions in GEOS-Chem, [http://acmg.seas.harvard.edu/geos/wiki\\_docs/emissions/megan.pdf](http://acmg.seas.harvard.edu/geos/wiki_docs/emissions/megan.pdf) , 2010.

Bergamaschi, P., R. Hein, M. Heimann, and P. J. Crutzen (2000a), Inverse modeling of the global CO cycle: 1. Inversion of CO mixing ratios, *J. Geophys. Res.*, 105, 1909–1927.

Bergamaschi, P., R. Hein, C. A. M. Brenninkmeijer, and P. J. Crutzen (2000b), Inverse modeling of the global CO cycle: 2. Inversion of  $^{13}\text{C}/^{12}\text{C}$  and  $^{18}\text{O}/^{16}\text{O}$  isotope ratios, *J. Geophys. Res.*, 105, 1929–1945.

Corbett, J. J., and H. W. Koehler (2003), Updated emissions from ocean shipping, *J. Geophys. Res.*, 108(D20), 4650, doi:10.1029/2003JD003751.

Dee, D. P., Uppala, S. M., Simmons, A. J., Berrisford, P., Poli, P., Kobayashi, S., Andrae, U., Balmaseda, M. A., Balsamo, G., Bauer, P., Bechtold, P., Beljaars, A. C. M., van de Berg, L., Bidlot, J., Bormann, N., Delsol, C., Dragani, R., Fuentes, M., Geer, A. J., Haimberger, L., Healy, S. B., Hersbach, H., Hólm, E. V., Isaksen, I., Kållberg, P., Köhler, M., Matricardi, M., McNally, A. P., Monge-Sanz, B. M., Morcrette, J.-J., Park, B.-K., Peubey, C., de Rosnay, P., Tavolato, C., Thépaut, J.-N. and Vitart, F. (2011), The ERA-Interim reanalysis: configuration and performance of the data assimilation system. *Quarterly Journal of the Royal Meteorological Society*, 137: 553–597. doi: 10.1002/qj.828

Eyring, V., Isaksen, I.S.A., Berntsen, T., Collins, W.J., Corbett, J.J., Endresen, O., Grainger, R.G., Moldanova, J., Schlager, H., and Stevenson, D.S. (2010), Transport impacts on atmosphere and climate: Shipping, *Atm. Env.*, 44, 4735 – 4771, doi:10.1016/j.atmosenv.2009.04.059, 2010.

Flemming, J., Inness, A., Flentje, H., Huijnen, V., Moinat, P., Schultz, M.G., and Stein, O. (2009). Coupling global chemistry transport models to ECMWF's integrated forecast system. *Geosci. Model Dev.*, 2, 253-265, doi:10.5194/gmd-2-253-2009.

Fortems-Cheiney, A., F. Chevallier, I. Pison, P. Bousquet, S. Szopa, M. N. Deeter, and C. Clerbaux (2011), Ten years of CO emissions as seen from Measurements of Pollution in the Troposphere (MOPITT), *J. Geophys. Res.*, 116, D05304, doi:10.1029/2010JD014416.

Granier, C., J.F. Lamarque, A. Mieville, J.F. Muller, J. Olivier, J. Orlando, J. Peters, G. Petron, G. Tyndall, S. Wallens, POET, a database of surface emissions of ozone precursors, available online at <http://www.aero.jussieu.fr/projet/ACCENT/POET.php> , 2005

Granier, C. et al. (2011). Evolution of anthropogenic and biomass burning emissions of air pollutants at global and regional scales during the 1980–2010 period, *Climatic Change*, doi: 10.1007/s10584-011-0154-1

Guenther, A., Karl, T., Harley, P., Wiedinmyer, C., Palmer, P.I., and Geron, C. (2006). Estimates of global terrestrial isoprene emissions using MEGAN (Model of Emissions of Gases and Aerosols from Nature), *Atmos. Chem. Phys.*, 6, 3181-3210.

Hollingsworth, A., et al. (2008). Toward a monitoring and forecasting system for atmospheric composition: The GEMS project. *Bull. Am. Meteor. Soc.*, 89, 1147-1164, doi:10.1175/2008BAMS2355.1

Hooghiemstra, P. B., M. C. Krol, P. Bergamaschi, A. T. J. de Laat, G. R. van der Werf, P. C. Novelli, M. N. Deeter, I. Aben, and T. Röckmann (2012), Comparing optimized CO emission estimates using MOPITT or NOAA surface network observations, *J. Geophys. Res.*, 117, D06309, doi:10.1029/2011JD017043.

Inness, A. et al. 2012. The MACC reanalysis: An 8-year data set of atmospheric composition. Submitted to ACPD

Kaiser, J. W., Heil, A., Schultz, M. G., Stein, O., van der Werf, G. R., Wooster, M. J., and Xu, W. (2011). Final report on implementation and quality of the D-FIRE assimilation system. MACC deliverable D D-FIRE 7, ECMWF.

Kaiser, J.W., Heil, A., Andreae, M.O., Benedetti, A., Chubarova, N., Jones, L., Morcrette, J.-J., Razinger, M., Schultz, M.G., Suttie, M., and van der Werf, G.R. (2012). Biomass burning emissions estimated with a global fire assimilation system based on observed fire radiative power. *Biogeosciences*, 9, 527–554, doi:10.5194/bg-9-527-2012.

Kasibhatla, P., A. Arellano, J. A. Logan, P. I. Palmer, and P. Novelli (2002), Top-down estimate of a large source of atmospheric carbon monoxide associated with fuel combustion in Asia, *Geophys. Res. Lett.*, 29(19), 1900, doi:10.1029/2002GL015581.

Kinnison, D.E., Brasseur, G.P., Walters, S., Garcia, R.R., Marsh, D.R., Sassi, F., Harvey, V. L., Randall, C.E., Emmons, L., Lamarque, J.F., Hess, P., Orlando, J.J., Tie, X.X., Randel, W., Pan, L.L., Gettelman, A., Granier, C., Diehl, T., Niemeier, U. and Simmons, A.J. (2007). Sensitivity of Chemical Tracers to Meteorological Parameters in the MOZART-3 Chemical Transport Model. *J. Geophys. Res.*, 112, D03303, doi:10.1029/2008JD010739.

Kloster, S., Feichter, J., Maier-Reimer, E., Six, K. D., Stier, P., and Wetzell, P.: DMS cycle in the marine ocean-atmosphere system – a global model study, *Biogeosciences*, 3, 29-51, doi:10.5194/bg-3-29-2006, 2006.

Lamarque, J.-F., Bond, T.C., Eyring, V., Granier, C., Heil, A., Klimont, Z., Lee, D., Liousse, D., Mieville, A., Owen, B., Schultz, M.G., Shindell, D., Smith, S.J., Stehfest, E., Van Aardenne, J., Cooper, O.R., Kainuma, M., Mahowald, N., McConnell, J.R., Naik, V., Riahi, K., and van Vuuren, D.P. (2010). Historical (1850-2000) gridded anthropogenic and biomass burning emissions of ozone and aerosol precursors: methodology and application. *Atmos. Chem. Phys.*, 10, 7017–7039, doi:10.5194/acp-10-7017-2010.

Lathière, J., D.A. Hauglustaine, N. De Noblet-Ducoudré, G. Krinner, G.A. Folberth (2005), Past and future changes in biogenic volatile organic compound emissions simulated with a global dynamic vegetation model, *Geophys. Res. Letters* 32, L20818, doi:10.1029/2005GL024164.

Miller, S. M., Matross, D. M., Andrews, A. E., Millet, D. B., Longo, M., Gottlieb, E. W., Hirsch, A. I., Gerbig, C., Lin, J. C., Daube, B. C., Hudman, R. C., Dias, P. L. S., Chow, V. Y., and Wofsy, S. C.: Sources of carbon monoxide and formaldehyde in North America determined from high-resolution atmospheric data, *Atmos. Chem. Phys.*, 8, 7673-7696, doi:10.5194/acp-8-7673-2008, 2008.

Moss, R.H., Edmonds, J.A., Hibbard, K., Manning, M., Rose, S. K., van Vuuren, D. P., Carter, T.R., Emori, S., Kainuma, M., Kram, T., Meehl, G., Mitchell, J., Nakicenovic, N., Riahi, K., Smith, S. J., Stouffer, R. J., Thomson, A., Weyant, J., Wilbanks, T. (2010), The Next Generation of Scenarios for Climate Change Research and Assessment. *Nature*. doi:10.1038/nature08823

Müller, J.-F., and T. Stavrou (2005), Inversion of CO and NO<sub>x</sub> emissions using the adjoint of the IMAGES model, *Atmos. Chem. Phys.*, 5, 1157–1186.

Ohara, T., Akimoto, H., Kurokawa, J., Horii, N., Yamaji, K., Yan, X., and Hayasaka, T. (2007), An Asian emission inventory of anthropogenic emission sources for the period 1980–2020, *Atmos. Chem. Phys.*, 7, 4419-4444.

Olivier, J.G.J., Van Aardenne, J.A., Dentener, F., Ganzeveld, L. and J.A.H.W. Peters (2005). Recent trends in global greenhouse gas emissions: regional trends and spatial distribution of key sources. In: "Non-CO<sub>2</sub> Greenhouse Gases (NCGG-4)", A. van Amstel (coord.), page 325-330. Millpress, Rotterdam, ISBN 90 5966 043 9.

Parrish, D. D. (2006), Critical evaluation of U.S. on-road vehicle emission inventories, *Atmos. Environ.*, 40, 2288–2300.

Pétron, G., C. Granier, B. Khatatov, J. Lamarque, V. Yudin, J. Müller, and J. Gille (2002), Inverse modeling of carbon monoxide surface emissions using Climate Monitoring and Diagnostics Laboratory network observations, *J. Geophys. Res.*, 107(D24), 4761, doi:10.1029/2001JD001305.

Pétron, G., C. Granier, B. Khatatov, V. Yudin, J.-F. Lamarque, L. Emmons, J. Gille, and D. P. Edwards (2004), Monthly CO surface sources inventory based on the 2000–2001 MOPITT satellite data, *Geophys. Res. Lett.*, 31, L21107, doi:10.1029/2004GL020560.

Riahi K, S Rao, V Krey, C Cho, V Chirkov, G Fischer, G Kindermann, N Nakicenovic, P Rafaj. 2011. RCP 8.5—A scenario of comparatively high greenhouse gas emissions. *Climatic Change*. 109:33-57. DOI 10.1007/s10584-011-0149-y.

Schultz, M. G., L. Backman, Y. Balkanski, S. Bjoerndalsaeter, R. Brand, J.P. Burrows, S. Dalsoeren, M. de Vasconcelos, B. Grodtmann, D.A. Hauglustaine, A. Heil, J.J. Hoelzemann, I.S.A. Isaksen, J. Kaurola, W. Knorr, A. Ladstaetter-Weissenmayer, B. Mota, D. Oom, J. Pacyna, D. Panasiuk, J.M.C. Pereira, T. Pulles, J. Pyle, S. Rast, A. Richter, N. Savage, C. Schnadt, M. Schulz, A. Spessa, J. Staehelin, J.K. Sundet, S. Szopa, K. Thonicke, M. van het Bolscher, T. van Noije, P. van Velthoven, A.F. Vik, F. Wittrock (2007): REanalysis of the TROpospheric chemical composition over the past 40 years (RETRO) — A long-term global modeling study of tropospheric chemistry, Final Report Jülich/ Hamburg, Germany, August 2007, published as report no. 48/2007 in the series „Reports on Earth System Science“ of the Max Planck Institute for Meteorology, Hamburg, ISSN 1614-1199

Shindell, D. T., et al. (2006), Multimodel simulations of carbon monoxide: Comparison with observations and projected near-future changes, *J. Geophys. Res.*, 111, D19306, doi:10.1029/2006JD007100.

Stein, O., Flemming, J., Inness, A., Kaiser, J. W., Schultz, M. G.: Global reactive gases and reanalysis in the MACC project, in press at *Journal of Integrative Environmental Science*, 2012.

Valcke, S., and Redler, R. (2006). OASIS4 User Guide (OASIS4\_0\_2). PRISM Support Initiative Report No 4, 60 pp.

van der Werf, G.R., Randerson, J.T., Giglio, L., Collatz, G.J., Mu, M., Kasibhatla, P.S., Morton, D.C., DeFries, R.S., Jin, Y., and van Leeuwen, T.T. (2010). Global fire emissions and the contribution of deforestation, savanna, forest, agricultural, and peat fires (1997–2009). *Atmos. Chem. Phys.*, 10:11707–11735.

van Vuuren, D.P., Edmonds, J., Kainuma, M., Riahi, K., Thomson, A., Hibbard, K., Hurtt, G. C., Kram, T., Krey, V., Lamarque, J.-F., Masui, T., Meinshausen, M., Nakicenovic, N., Smith, S.J., Rose, S.K. (2011). The representative concentration pathways: an overview. *Climatic Change*, 109, 5–31, doi:10.1007/s10584-011-0148-z.

**KEYWORDS**

Carbon monoxide, MACC, emission inventories, ACCMIP